Engineering Geology 328 (2024) 107382

Contents lists available at ScienceDirect

Engineering Geology

journal homepage: www.elsevier.com/locate/enggeo

Implementing close-range remote surveys for the digitally supported rock mass stability analysis

S. Mineo, D. Caliò, G. Zocco, G. Pappalardo *

Department of Biological, Geological and Environmental Sciences, University of Catania, Corso Italia 57, Catania, Italy

ARTICLE INFO

Keywords:
Rockfall
UAV photogrammetry
Stability analysis
Trajectory simulation

ABSTRACT

A digitally supported rock mass stability analysis is herein presented for the implementation of non-contact close-range remote surveys against landslide hazard in sheltered environments, such as Marine Protected Areas. An airborne photogrammetric survey was carried out at the Lachea Islet (Sicily), which is part of a small volcanic archipelago with a peculiar geological history, hosting unstable rock masses belonging to the first eruptive stages of Mount Etna. The digital model built for this study allowed extracting the discontinuity orientation data, performing a kinematic analysis along the recognized discontinuity clusters, and quantifying the volume of potentially unstable boulders. Laboratory tests allowed achieving the main physical-mechanical parameters of involved rocks, which were used to perform a quantitative stability analysis under both deterministic and probabilistic approaches, based on the extracted digital data. Finally, a 3D rockfall trajectory analysis was carried out by simulating statistical rockfall path on the digital model built for the study. Results highlighted a poor stability in the studied islet sector, which is worsened by taking into account the high seismicity that characterizes the area. The main tourist elements of the islet must be considered at risk, as they are located within the simulated trajectories of the landslides. The methodological protocol carried out for this study, based on conventional procedures but using remotely derived and digitally processed information, can be considered a useful tool in the frame of nature-based solutions for hydro-meteorological hazards connected to climatic changes.

1. Introduction

With climate change, the hydro-meteorological hazard represents a topic gaining more and more attention by the scientific community, due to its strong relationship with the risk arising from extreme natural phenomena (Quevauviller and Gemmer, 2015). Among these, landslides are usually caused by the combination of hydro-meteorological and geological factors, and their socio-economic impact due to climatic change involves a high level of uncertainty (Casagli et al., 2017b). Coastal cliffs, for example, provide a high landscape value to many natural sites worldwide (Young, 2018; Morales et al., 2021), although being affected by an extreme fragility. Marine processes play a direct action on the rock face, with waves impacting and abrading the rock, and progressively giving rise to retreat phenomena (Rosser et al., 2013; Young, 2018). Mechanical and chemical weathering, along with rainfalls, adversely affect the rock engineering geological properties, favoring the strength reduction and increasing the predisposition of the cliff to failures (Porter and Trenhaile, 2007; Collins and Sitar, 2008; Barbano et al., 2014). In this setting, rockfalls are one of the major natural hazards affecting coastal cliffs (Marques, 2008; Calista et al., 2019; Benjamin et al., 2020; Daniela et al., 2020), and they represent a security management issue connected to the climate change.

The goal of this paper is the establishment of a non-invasive close-range remote surveying procedure applied to the rock mass stability analysis in a Marine Protected Area (MPA), which represents a sheltered location "by law or other effective means to protect part or all of the enclosed environment" (Humphreys and Clark, 2020; Kriegl et al., 2021). The area chosen for this study is the Lachea Islet, located within the "Lachea Islet and Cyclop Rocks" MPA in Sicily (southern Italy). It is part of a small archipelago with a series of sea rocks resulting from the first eruptive phases of Mount Etna, which is acknowledged among the UNESCO World Heritage List. The technical issue of this study is that both the Lachea Islet and the near sea rocks suffer from rockfall instability phenomena, also enhanced by the peculiar geological and tectonic setting (Pappalardo et al., 2021). This is why the disembarkation on the islet is currently prohibited, and the MPA restrictions force to maintain a very low invasiveness level for the engineering geological characterization of the cliffs. In this regard, the international scientific community

* Corresponding author.
E-mail address: pappalar@unict.it (G. Pappalardo).

https://doi.org/10.1016/j.enggeo.2023.107382
Received 18 May 2023; Received in revised form 5 December 2023; Accepted 5 December 2023
Available online 8 December 2023

has been working on new technical approaches, mostly relying in non-contact surveys and digital analyses, to achieve reliable tools to model the rock mass stability. Among the used technologies, laser scanning, infrared thermography imaging and photogrammetry can be acknowledged (Abellán et al., 2006; Salvini et al., 2017; Macciotta et al., 2020; Gallo et al., 2021; Mineo et al., 2021; Marija et al., 2022; Nikolakopoulos et al., 2022; Vivaldi et al., 2023; Kong et al., 2021). At nature reserves, Caliò et al. (2023a) exploited the combination between infrared thermography and digital photogrammetry by UAV (Unmanned Aerial Vehicle) to evaluate the rockfall magnitude at a sub-vertical cliff, while Clemente et al. (2023b) and Zhang et al. (2022) elaborated models obtained by terrestrial laser scanners and unmanned vehicles to simulate rockfall trajectories and evaluate their runout and energy at a coastal site in Spain. Other case studies involve the use of LiDAR (Light Detection And Ranging) data to build detailed Digital Terrain Models and simulate rockfalls in a MPA of Italy (Clemente et al., 2023a). Similarly, Morales et al. (2021) recognized the main instability features at a geopark area by exploiting UAV photogrammetric data with the derived orthomosaics and geoid corrected Digital Terrain Models. In this paper, the technical protocol is organized along a methodological path that covers all the stages of a conventional rock mass study but with data remotely collected by UAV photogrammetry and exploited in the form of a digital 3D rock mass model. This model is used for the extraction of discontinuity orientation data, which were statistically processed to shed light on the most recurring unstable kinematic failure patterns. Based on the digitally derived data, the numerical stability analysis was performed according to both deterministic and probabilistic approaches, widely used in the literature (Gilham et al., 2019; Wang et al., 2023). In the first case, the Factors of Safety (FoS) along the kinematically unstable discontinuity planes were estimated, while the probabilistic analysis led to the calculation of the related Probability of Failure (PoF). Input data on the physical-mechanical properties of the rock types and discontinuity shear strength were supported by laboratory tests. Then, the digital computation of the most recurring rock volumes, to be referred as potential detaching blocks, was carried out and 3D rockfall trajectory simulations were performed on the realistic digital terrain model built from UAV data.

2. Geological setting of the study area

The study area is located in the Ionian Sea, along the eastern coastline of Sicily (Italy), where a small archipelago with a series of sea rocks and an islet is found. From the geological point of view, the archipelago hosts volcanic rock outcrops locally covered by marly sediments (Fig. 1a). Its origin is due to the initial activity of Mount Etna, the highest active volcano in Europe, which is now part of the UNESCO World Heritage List for its cultural, natural and scientific relevance. Between 500 and 330 ky ago, in a submarine environment, a molten magma body intruded into the seafloor (Early-Middle Pleistocene marly clays), where it started cooling (Fig. 1b). Then, the tectonic uplift led to the emersion of the volcanic body, which currently hosts the older marly rocks on its top as remains of the ancient seafloor sediments; moreover, the wave erosion processes have shaped the Lachea islet and the surrounding sea rocks into the current landscape (Tanguy et al., 1997; Branca et al., 2008) (Fig. 1c).

The major fracture systems of the rock masses are linked to the cooling process of the volcanites, which are characterized by a suggestive columnar jointing (Fig. 1d). At the time of its formation, this jointing arrangement was transferred to the encasing marly rocks, which now show a fracture system consistent with that of the underlying volcanic rock masses. The study area is also tectonically active, being crossed by WNW-ESE trending tectonic segments affecting both the emerged and submerged lands (Cavallaro, 2010; Bonforte et al., 2011; Barreca et al., 2018; Cristofolini et al., 1987) (Fig. 1a). Similarly oriented persistent discontinuity segments recur along the Lachea Islet, and their presence is highlighted by small canyons and/or wide fractures. These affect both the volcanic rock masses, where are well developed, and the marly outcrops, where these are arranged in subparallel, closely spaced, fracture systems, likely due to the more plastic behavior of this rock type under stress (Fig. 1e). Moreover, at a larger scale, regional normal-oblique faults are responsible for the uplift affecting the south-eastern coastal sector of Mount Etna (Branca et al., 2014). From this setting, it can be deduced that the study area is affected by a high seismic activity, with frequent earthquakes that can be related to both regional and local seismogenic sources and that historically reached moderate to high magnitudes (Barbano et al., 2014).

3. Methods

3.1. Workflow

The methodological workflow designed for this study is developed along two main technical branches, focused on the rock characterization at both laboratory and field scale (Fig. 2). In the first branch, the intact rock laboratory characterization was aimed at assessing the main engineering geological properties of the two lithotypes outcropping on the islet, i.e., volcanites and marls, as well as the shear strength along discontinuities. To this purpose, NX cylindrical specimens were cored from blocks sampled in the field and underwent, after a preliminary description at the hand-scale, a series of physical-mechanical tests to estimate their bulk and real density, total porosity, Uniaxial Compressive Strength (UCS) and Young's Modulus (E), according to the international EN1936, ASTMD2938 and ISRM (2007) guidelines. Before compression tests, the same specimens were employed to estimate the basic friction angle (ϕ_b) along discontinuities through a series of tilt tests in a core-based configuration (Stimpson, 1981).

The second branch of the methodological approach (Fig. 2) is based on the field rock mass survey, which was carried out by an aerial photogrammetry surveying campaign. Field data were also conventionally surveyed at representative available outcrops for the photogrammetric data validation. The UAV survey was extended to the whole north-western sector of the islet, where the major elements at risk are present (disembarkation spots, a tourist path, and a museum). This allowed covering also high rock mass portions, which could not be directly reached by field operators for conventional surveys. The photogrammetric-derived 3D model was further processed to gather quantitative data on the spatial attitude of the main discontinuities crossing the rock masses (Fig. 2). This allowed collecting a statistically reliable amount of data to be used for kinematic analysis. Furthermore, the combination between the recognized kinematically unstable failure patterns and the rock properties allowed carrying out a numerical stability analysis for the estimation of the Factors of Safety (FoS), under both static and pseudostatic condition, related to each critical pattern highlighted by the kinematic analysis (Fig. 2). Estimated FoS were also analyzed from a statistical point of view to estimate the Probability of Failure (PoF) related to the unstable discontinuity sets. Simultaneously, the discontinuities recognized on the digital rock mass model allowed defining the volumes of key representative unstable rocks, which were geometrically defined and numerically quantified on the point cloud. This volumetric datum was used as input variable to model the trajectory of potential rockfalls, which were simulated on the built 3D islet model to highlight the potential impact on the elements at risk.

3.2. Methodological focus on airborne photogrammetry and discontinuity data extraction

Photogrammetric data were collected at the most exposed to rockfall risk islet sector, where the disembarkation area and the tourist paths are threatened by rock mass instability. The used UAV is a DJI Mavic2Pro, a multirotor drone equipped with a 20 Mpixel optical camera with a 1" CMOS digital sensor. The flight plan was set to maintain a constant Ground Sample Distance (GSD) and a 70–80% overlap rate between the

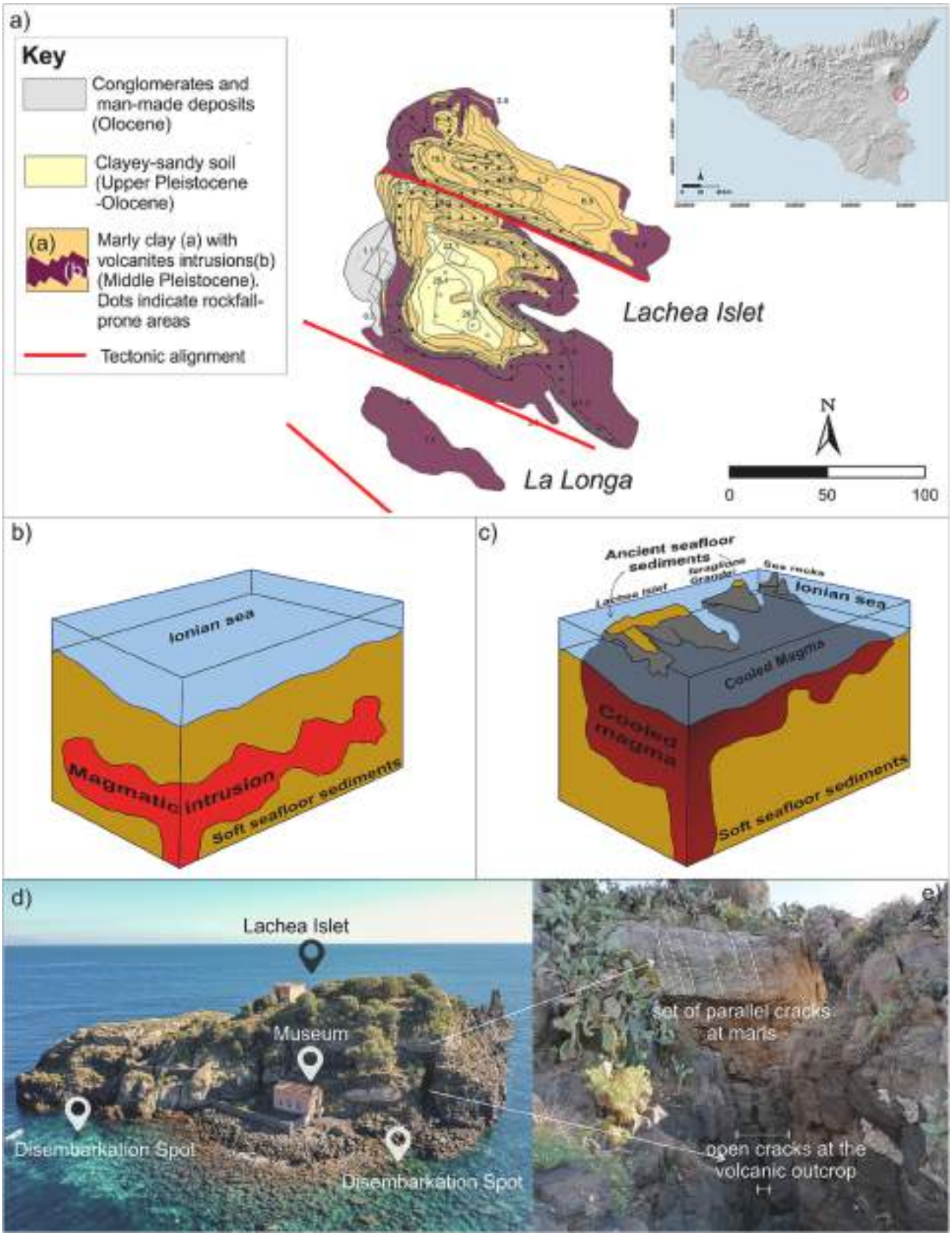

Fig. 1. a) geological map of the Lachea Islet and Cyclop Rocks (modified after Pappalardo et al. (2021)); b) simplified model of the initial stage of magma intrusion at the study area; c) simplified model of the archipelago formation; d) view of Lachea Islet; e) focus on the discontinuity development at volcanic and marly outcrops.

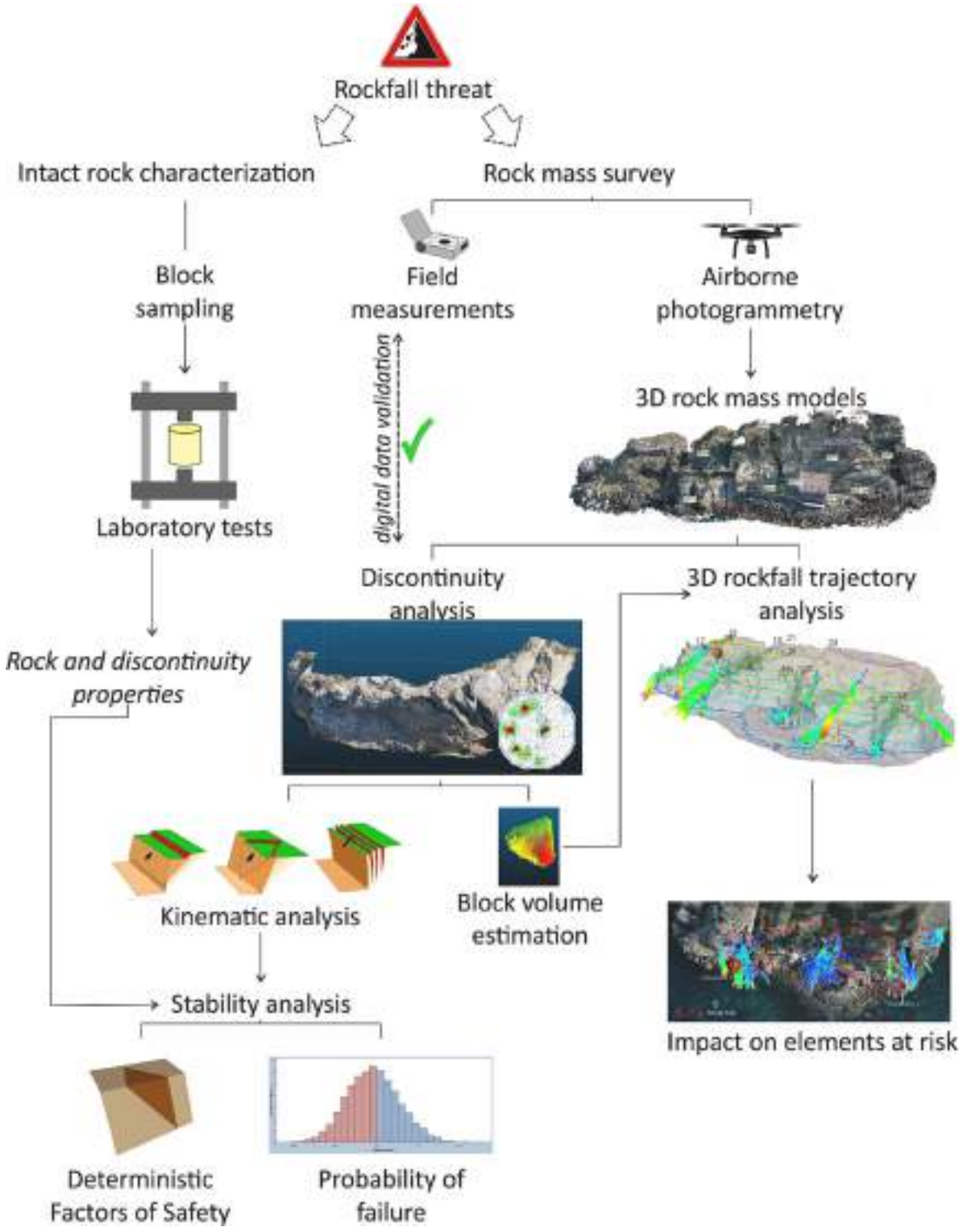

Fig. 2. Methodological workflow of the study.

acquired frames. According to Tu et al. (2021), two different flights were carried out in order to achieve a good-quality photogrammetric reconstruction and data redundancy. In particular, the first flight was operated in manual mode, with the camera optical axis trim varying from 0° to 45° with respect to the horizontal. This ensured the detailed framing of the vertical rock faces, along with an optimal definition of slope sectors with inclination between 35° and 60°. The second flight was an automated Nadiral flight for the optimal location of 11 ground targets, homogeneously distributed within the surveyed area, as well as for a more accurate photogrammetric reconstruction. The survey covered a 3720 m^2 area and returned 458 images that were aligned by maintaining an average flight altitude of 20 m. As a result, a digital model of the surveyed islet sector was produced with a 5 mm/pixel ground resolution, in terms of GSD.

The images' post-processing was performed through Structure from Motion (SFM) algorithms (James and Robson, 2012; Westoby et al., 2012; Fonstad et al., 2013), which are based on sophisticated Computer Vision set of rules that use 2D images acquired from different viewpoints

to reconstruct the three-dimensional geometry of an object (Tonkin and Midgley, 2016). More specifically, the procedure was divided into four steps: 1) image import and alignment to generate a sparse point cloud of 207,000 points; 2) geographic coordinates set on ground targets for georeferencing and scaling the model; 3) processing of a 167,000 points dense cloud; 4) production of a 3D polygonal mesh i.e., a set of polygons that are connected together to form a continuous surface.

The built digital model of the islet rock masses was analyzed with the aim of retrieving spatial orientation discontinuity data, which is the first step towards a digitally supported stability analysis. In particular, the orientation data were extracted through the semiautomatic approach based on the Scalar Field function, which proved a reliable tool in similar literature studies (e.g., Sturzenegger and Stead, 2009; Casagli et al., 2017a; Colica et al., 2021; Mineo et al., 2022). It allows the conversion of the normal vector to a specific point, which can be displayed through a color ramp. For this study, the dip/dip direction value was set as a scalar field and then digital extraction of data was carried out through the open source CloudCompare program (CloudCompare 2.12.4), which allowed handling about 800 orientation data at 11 selected surveying windows. For selected blocks, the corresponding volume was estimated to provide a reference for the rockfall trajectory simulations described in the following sections. In particular, the tool "Compute 2.5D volume", found in the open-source software Cloude Compare, was used. It allows calculating the relative difference between a reference plane, rasterized in the dense point cloud, and the identified boulder surface that is then turned into a volume value (Wheaton et al., 2009; Caliò et al., 2023a).

3.3. Methodological focus on stability analysis

Based on the major kinematic instability features defined by the joint set geometrical relationship with the slope face, the stability analysis was carried out by the Limit Equilibrium method (Hoek and Bray, 1981; Wyllie and Mah, 2014) implemented in the RocScience software suit. For the planar sliding failure pattern, the deterministic estimation of FoS is carried out by resolving all forces acting on the slope into component parallel and normal to the sliding plane, which is assumed parallel to the slope face. The vector sum of the shear forces is referred to as "driving force", while the product of the total normal forces and the tangent of the friction angle, plus the cohesive force, is termed "resisting force". The FoS of the sliding block is the ratio of the resisting force to the driving force. For wedge sliding, FoSs were calculated according to Hoek (1973), who takes into account the friction angles and cohesive forces along both the intersecting discontinuity planes based on the assumption that the full shear strength is mobilized simultaneously. In this case, the intersection between the failure planes is validated in order to achieve a reliable wedge geometry. For toppling failure, the analysis relies on the relationship between the friction angles on the sides and base of the unstable blocks: FoS results by dividing the tangent of the friction angle believed to apply to the rock layers, by the tangent of the friction angle required for equilibrium (Goodman and Bray, 1976). For these three major failure patterns, FoS was calculated under both static and pseudo-static conditions, due to the high seismicity of the study area. In particular, the effect on stability played by the seismic ground motion is calculated by simulating a static force acting in direction out of the slope face.

Nevertheless, since the deterministic analysis is carried out on single fixed values of representative orientation and strength parameters, this approach is unable to account for variation in rock mass properties and conditions (Park et al., 2005). To overcome this technical limitation, the stability analysis was carried out even according to a probabilistic approach, which allows considering the statistical variability of orientation and strength discontinuity parameters. Each parameter is considered as a random variable, and the analysis, involving different values for each datum, will result in different FoSs. In this case, the Monte Carlo simulation method allowed estimating the PoF for 5000 iterations by processing the input kinematic and kinetic analysis data (Radhi et al., 2008). The overall PoF is a conditional probability, resulting from the product of the kinematic probability and the kinetic probability (Einstein, 1996; Budetta and De Luca, 2015).

3.4. Methodological focus on rockfall trajectory analysis

Once that (1) the instability condition characterizing the surveyed rock masses were ascertained, (2) the volumes of potential detachments were calculated, and (3) the rock physical parameters were estimated, a rockfall trajectory analysis was carried out by simulating the path of potential rockfalls crossing the key spots of the study area. The purpose of this analysis is to turn into a practical outcome the digital stability assessment that was performed, to consider possible hazardous scenarios in the frame of a risk management activity. Rockfall paths were simulated by RocFall 3D (Rocscience), which is a three-dimensional statistical analysis program designed to assess the runout distance on the 3D slope geometry, and to determine energy, velocity and bounce height of falling blocks along multiple paths. The advantage of simulating rockfall trajectories in a 3D environment is that the block lateral variation, which is affected also by the slope morphology, can be documented (Agliardi and Crosta, 2003; Dorren et al., 2006; Caviezel et al., 2019; Noël et al., 2022; Akin et al., 2021; Yan et al., 2023). The analysis method applied herein is the Lumped Mass, which assumes a falling rock as an infinitesimal particle with a mass and a velocity (Hoek, 1987). Simulations were performed by considering a block mass compatible to the estimated rock volumes, and the ground morphology was imported by the dense point cloud used for the digital rock mass analysis. A couple of coefficients of restitution was assigned to the ground according to the outcropping material. In particular, four main material categories were set: bare rock, at bare rock mass outcrops; bare blockfield, at the small beach where the surface is covered by block-sized angular rocks; rock debris, and gravel road at the tourist path (Table 1). Rockfall seeders were placed at the potential source areas located on the digital model, and 50 trajectories were simulated by the Monte Carlo sampling method to take into account the rockfall variability. For each simulated path, the runout distance and impact points were analyzed, in order to assess the potential rockfall impact on the elements at risk.

4. Intact rock and discontinuity characterization

From the hand scale analysis, collected volcanic rock specimens are characterized by a micro-vesicular structure, with homogeneously distributed millimeter-sized vesicles. Although this textural feature is common among the volcanic products of Mount Etna, the peculiarity of the rocks sampled on the Lachea islet is that vesicles are often filled with yellowish clayey-marly material, entrapped during the volcanic body intrusion in the ancient sea floor (Fig. 3a). From the physical point of view, tested rocks are characterized by a 5% average total porosity and a 2.6 g/cm^3 bulk density, which are values typical of Etna's massive lavas, according to the literature knowledge (Pappalardo et al., 2017; Pappalardo and Mineo, 2017). On the contrary, UCS and E values ranges from 87.3 to 97.3 MPa and from 8.5 and 9.8 GPa, respectively, proper of

Table 1
Coefficients of restitution considered for the simulation model.

Authors	Material Type	R_n	R_t
(Pfeiffer and Bowen, 1989)	Rock debris	0.315 ± 0.005	0.850 ± 0.007
RocFall3 repository (RocScience)	Gravel Road	0.35 ± 0.04	0.85 ± 0.04
(Pfeiffer and Higgins, 1990)	Bare rock	0.35 ± 0.04	0.85 ± 0.04
RocFall3 repository (RocScience)	Blockfield	0.50 ± 0.06	0.70 ± 0.06

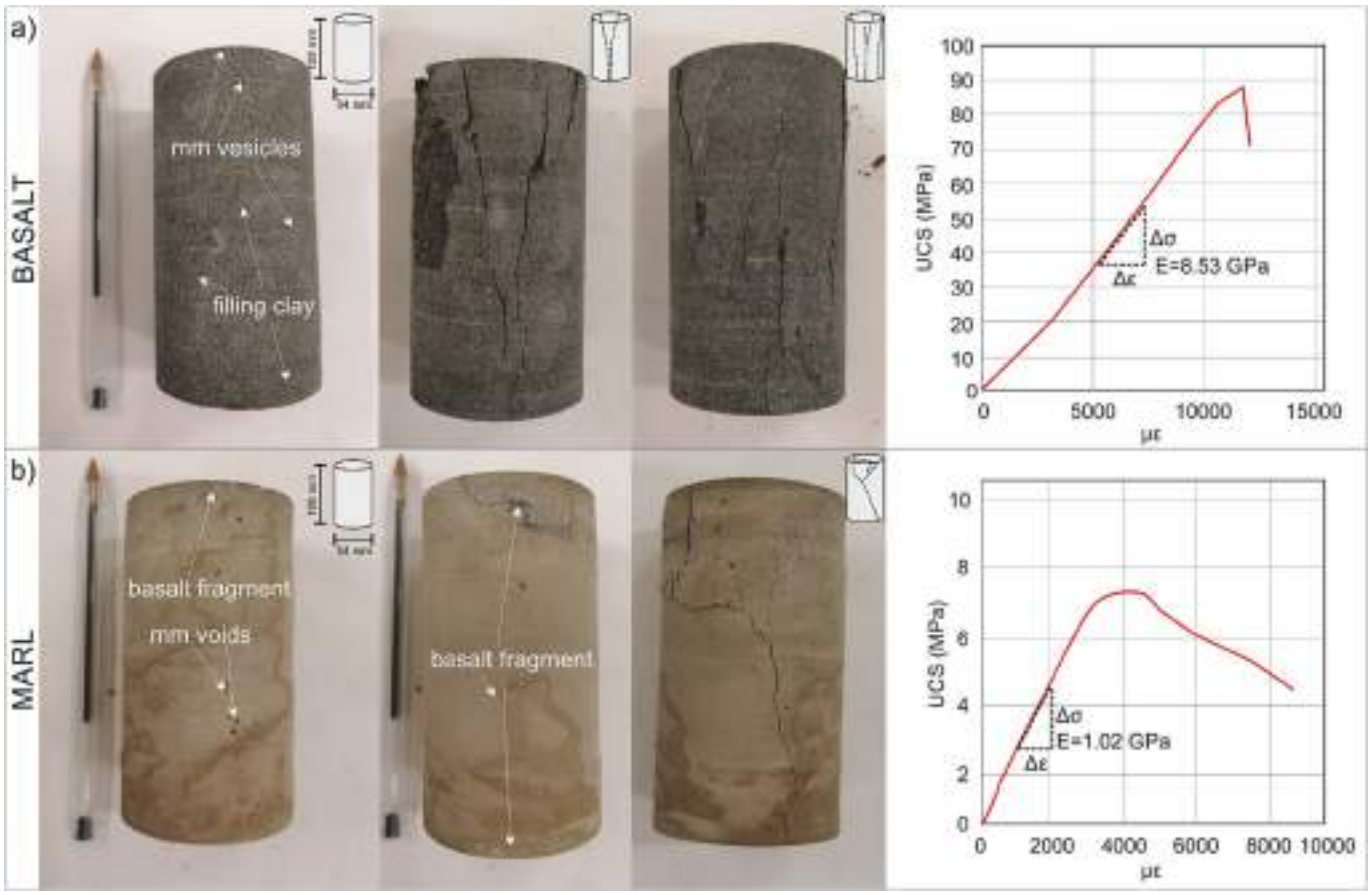

Fig. 3. Representative pre- and post-failure specimens of tested lavas (a) and marls (b) with a representative stress-strain curve resulting from uniaxial compression tests.

millimetric-vesicular volcanic rocks. This dissonance is likely due to de presence of clayey material filling the millimetric rock vesicles, which, on the one hand reduces the rock porosity and increases its bulk density. On the other hand, this filling material does not offer any adjunctive mechanical resistance, thus keeping UCS and E values within the common ranges of millimetric-vesicular lavas. The rock failure mode under uniaxial loading is a combination of axial splitting and Y-shaped failure, mainly related to the development of one or more major cracks in the direction of the applied load (Basu et al., 2013; Pappalardo et al., 2016). From the discontinuity point of view, ϕ_b, experimentally estimated through tilt tests, ranges between 32° and 35°. These values fall within the ϕ_b ranges available in the literature and referring to the same rock type (e.g., Alejano et al., 2012; Zhang et al., 2019).

Marly rocks cannot be defined as marls *stricto* sensu, since heterometric volcanic clasts are embedded in a clayey matrix. These clasts are millimetric to centimetric in size, and they cause a relevant heterogeneity of the rock texture at the hand scale (Fig. 3b). To coring, the rock is soft to strong, based on the occurrence of these volcanic fragments. Moreover, locally, millimetric voids occur, especially at the volcanic clasts, and marls show a brecciated aspect. The mean bulk density value is 1.5 g/cm^3 and total porosity is, on average, 26%, while UCS and E are around 7.6 MPa and 1.0 GPa, respectively, to be considered indicative of a highly heterogeneous and peculiar rock type, where the variable content of volcanic fragments can cause changes in its engineering geological properties. Under uniaxial compression, marls failed through a shear fracturing pattern, a way between brittle failure and ductile deformation (Fig. 3b). This mode of failure could be related to the coalescence of smaller axial cracks (Basu et al., 2013) which is likely enhanced herein by the presence of pre-existing discontinuities represented by the boundary between the volcanic fragments and the marly matrix.

From the discontinuity point of view, the performed tilt tests returned lower ϕ_b than those achieved for volcanites, which are between 24° and 29°.

5. Digital rock mass discontinuity analysis

The discontinuity data were extracted from the 3D model at 11 surveying windows, from 32 to 75 m^2 wide, located at both marl (7 windows) and volcanite (3 windows) outcrops. Their location was chosen based on the major elements at risk distribution (i.e., tourist path, disembarkation points, museum, beach) and on the evidence of instability (Fig. 4a). Discontinuity data were plotted on stereograms to analyze their statistical occurrence in terms of spatial orientation and relationship with the slope face. Four to five main sets are recognized at each surveying window, for a total of 8 families (Fig. 4b). The average number of poles used to recognize the discontinuity sets is 11. This value is averaged by considering the maximum of 40 poles, obtained for the most visible sets. Moreover, the minimum value of 4 poles obtained for the less visible sets to the UAV camera underlines that the number of surveyed poles is strongly dependent on the exposure of the discontinuity plane with respect to the dense point cloud. Nevertheless, the redundance of values at each surveying spot allowed us to recognize also those sets showing un unfavorable orientation with respect to the UAV camera. The kinematic analysis, performed by conservatively considering the lowest ϕ_b estimated for the two lithologies, showed that the most recurring failure patterns are planar sliding, wedge sliding and toppling. Planar sliding is mainly enhanced along those planes belonging to Set 1 when the slope face dips towards West, and along Sets 8 and 7 for slope walls dipping towards Southwest and Northwest,

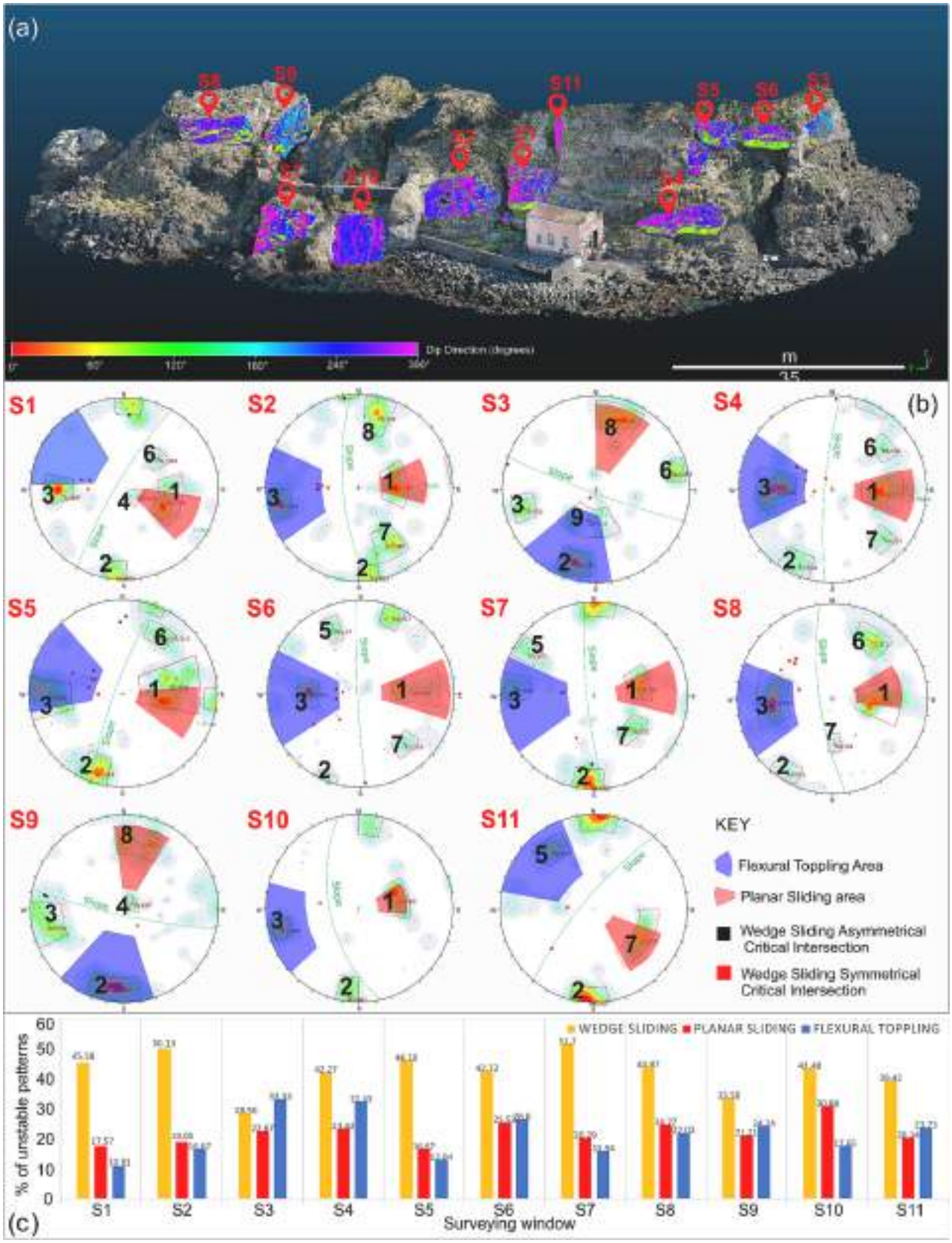

Fig. 4. a) 3D model of the western sector of Lache Islet, with location of the 11 surveying windows in scalar field mode; b) stereograms of extracted discontinuity data and kinematic analysis; c) percentage of unstable failure patterns at each surveying window.

respectively (Fig. 4b). The average percentage of poles falling within the critical area for planar sliding is 22%, with a 31% maximum found at the S10 surveying window (Fig. 4c). Wedge sliding occurs according to both symmetrical and asymmetrical configurations. In the first case, the intersection of discontinuity planes gives rise to a rock volume sliding along the intersection line, while for asymmetrical wedges the sliding occurs along one of the planes. By considering all the intersecting surveyed discontinuity planes, the average percentage of the unstable intersections is 42.5%. Flexural toppling mainly occurs along Set 3 when the slope face dips towards West, while occasionally also Sets 2, 5 and 9 are involved with an overall 21.5% mean percentage of unstable poles (Fig. 4b-c).

By further analyzing the stereograms, the systematic recurrence of three main discontinuity sets can be highlighted. These are Sets 1–2 and 3, with set 2 characterized by an orientation parallel to the fault segments crossing the islet.

6. Stability analysis

According to the Limit Equilibrium method, the numerical stability analysis was carried out by taking into consideration only the discontinuity sets that resulted unstable from the kinematic point of view (Fig. 4). The first step of this analysis, aiming at quantifying FoS and PoF under static and pseudostatic conditions, was the preliminary modeling of the kinematic patterns. In particular, the kinematically unstable discontinuity sets were recognized on the dense point cloud and one or more representative failure planes were rasterized (Fig. 5). The corresponding pattern was modeled by the RocScience suite for stability analysis, and reliable simplified models were achieved (Fig. 5). Based on the average orientation data resulting from the stereonet analysis, as

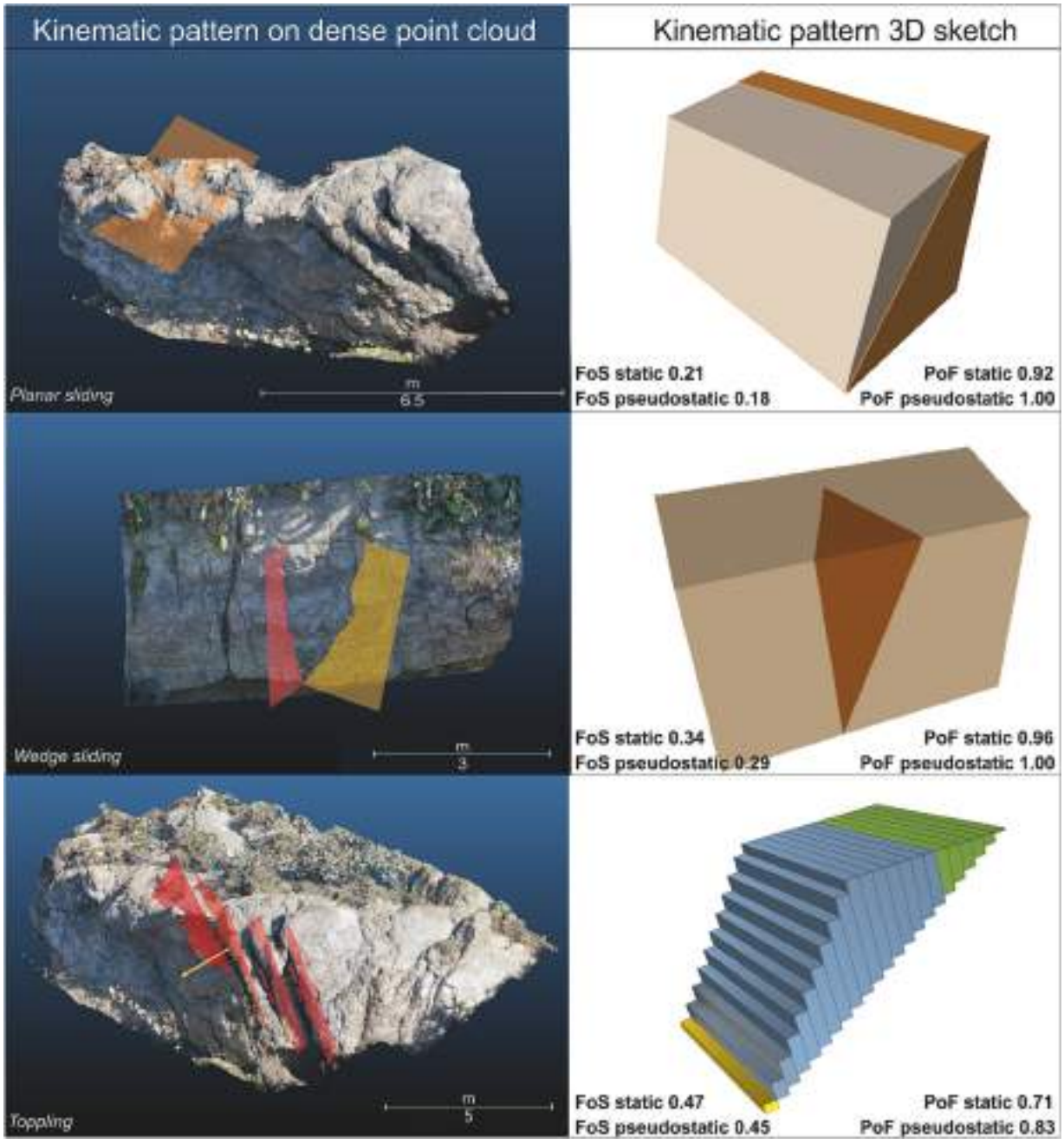

Fig. 5. Examples of a comparison between a digital failure pattern recognized on the dense point cloud (the arrows indicate the normal vector to the rasterized planes), and the 3D sketch built for the stability analysis.

well as on the statistical variability affecting each discontinuity set, different ranges of FoS and PoF resulted from the analysis. Friction along discontinuity was modeled according to the Mohr-Coulomb shear strength model, by assuming a conservative zero cohesion (discontinuity are actually not cemented and no potential occurrence of rock bridges was considered) and the lowest ϕ_b value obtained by tilt tests with respect to the deterministic approach. Zero cohesion and the range of obtained ϕ_b in a statistically normal distribution were considered for the probabilistic approach. The choice of using these parameters is conservative, since the discontinuities surveyed in the field at the validation spots showed a smooth to slickenside surface. From a general point of view, estimated FoS are averagely below the limit equilibrium (FoS < 1), and PoF are averagely >0.5 (Fig. 6); this is because the numerical analysis was carried out only on the kinematically unstable discontinuities, which represent the most critical systems from the stability point of view. It must be underlined that this conservative analysis approach does not consider the potential occurrence of rock bridges or joint cementation, which are not detectable at the current scale and by the surveying methodology. These, if present, would locally increase the cohesion along the discontinuity surfaces favoring the resisting forces, thus the stability. Planar sliding is the only pattern characterized by few stable cases, with 1.37 and 1.16 maximum FoSs under static and pseudostatic modeling, respectively. This is because some discontinuity sets (e.g., sets 1–4-8) can be considered borderline from the kinematic stability point of view (Fig. 4). This is why the analysis was carried out by taking into account all the poles of surveyed discontinuities, rather than only a representative mean plane. The seismic action causes a 11.6% mean reduction of the FoS value. In a specular wave, planar sliding resulted the failure pattern characterized by the widest range of PoF, although the average of resulting data is close to 1 (Fig. 6). In this case, the difference between static and pseudostatic condition is slight (about 1.5%).

The stability of the modeled wedge sliding cases is characterized by FoS values always below the limit equilibrium, ranging from a minimum of 0.1 to a maximum of 0.94. When the seismic action is included in the computation, the average FoS for this patter is reduced of about 10%. Wedge failure PoFs are >0.5, with the highest mean value (0.89%) referring to the pseudostatic conditions.

Finally, toppling resulted the most unstable pattern from the limit equilibrium point of view, with a negligible variation of the average FoS (0.35) from static to pseudostatic condition. On the other hand, mean PoF values are comparable to those affecting wedges, although with a slightly narrower range.

7. Rockfall trajectory analysis

The statistical simulation of rockfall trajectories was based on the preliminary identification of potential source areas at the islet sectors hosting the main elements at risk. For each source area, the likely detachable volume was calculated on the digital model (Fig. 7a). Volumetric values range from a minimum of 0.01 to a maximum 1.2 m^3. The model used for rockfall simulation resulted from the triangulation of the original dense point cloud, which was properly resampled, achieving a mesh that faithfully represents the real morphology of the area. At the northern sector of the islet, rockfalls threat a disembarkation spot, with all the simulated trajectories reaching the sea (Fig. 7b). The block movement shows an initial path characterized by numerous impacts with the slope, probably due to rolling action, and proceeds downstream through rebounds and free fall according to the impact point heatmap, which shows the contact points of the rocks on the slope (Fig. 7c). At the middle sector, rockfalls threat part of the tourist path and the museum. More specifically, most of the simulated falling blocks would reach and stop at the museum entrance with potential damages to the structure and a high risk in case of human presence (Fig. 7b). Few boulders reached also a small rocky beach, seasonally occupied by numerous bathers reaching the islet by swimming. In this case, most of the impacts between block and slope occur at both the higher slope sectors and at the museum entrance, where the flat morphology favours the rock rebound and roll (Fig. 7c). At the southern sector, the main threat is posed to the other disembarkation spot, part of the small beach and a seas strip usually snorkelling destination. The impact point location shows that most of the boulder would reach these elements at risk (Fig. 7b-c).

8. Discussion and conclusions

Results achieved by this study allow discussing two different aspects referring to both the local case of the Lachea MPA and the scientific approach that was carried out, and that could be adapted to numerous other contexts worldwide.

Starting from the first discussion hint, the MPA rock mass stability is conditioned by key discontinuity sets, which recur within the whole surveyed islet sector and that are linked to the major tectonic lines. One of this is mainly oriented WNW-ESE, and its occurrence is marked by small canyons and/or wide fractures at the islet rock mass, which were well recognized in the digital model built for this study. This aspect, besides further proving the link between landslide and tectonics already pointed out in the published literature (Willenberg et al., 2008; Tokiwa et al., 2011), suggests that the tectonic activity of an area is a key knowledge element to take into consideration when dealing with similar studies. In fact, the presence of fault systems could be considered a

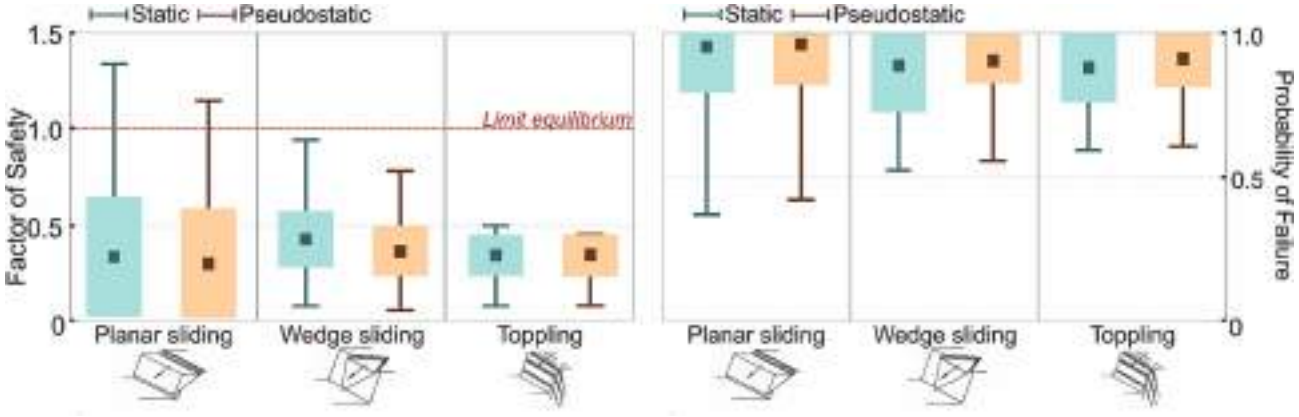

Fig. 6. Statistics of Factor of Safety (FoS) and Probability of Failure (PoF) resulting from the numerical stability analysis computed for planar sliding (15 cases), wedge sliding (29 cases) and toppling (12 cases). Boxes indicate the standard deviation, whiskers indicate the minimum and maximum values, squares are for the mean value.

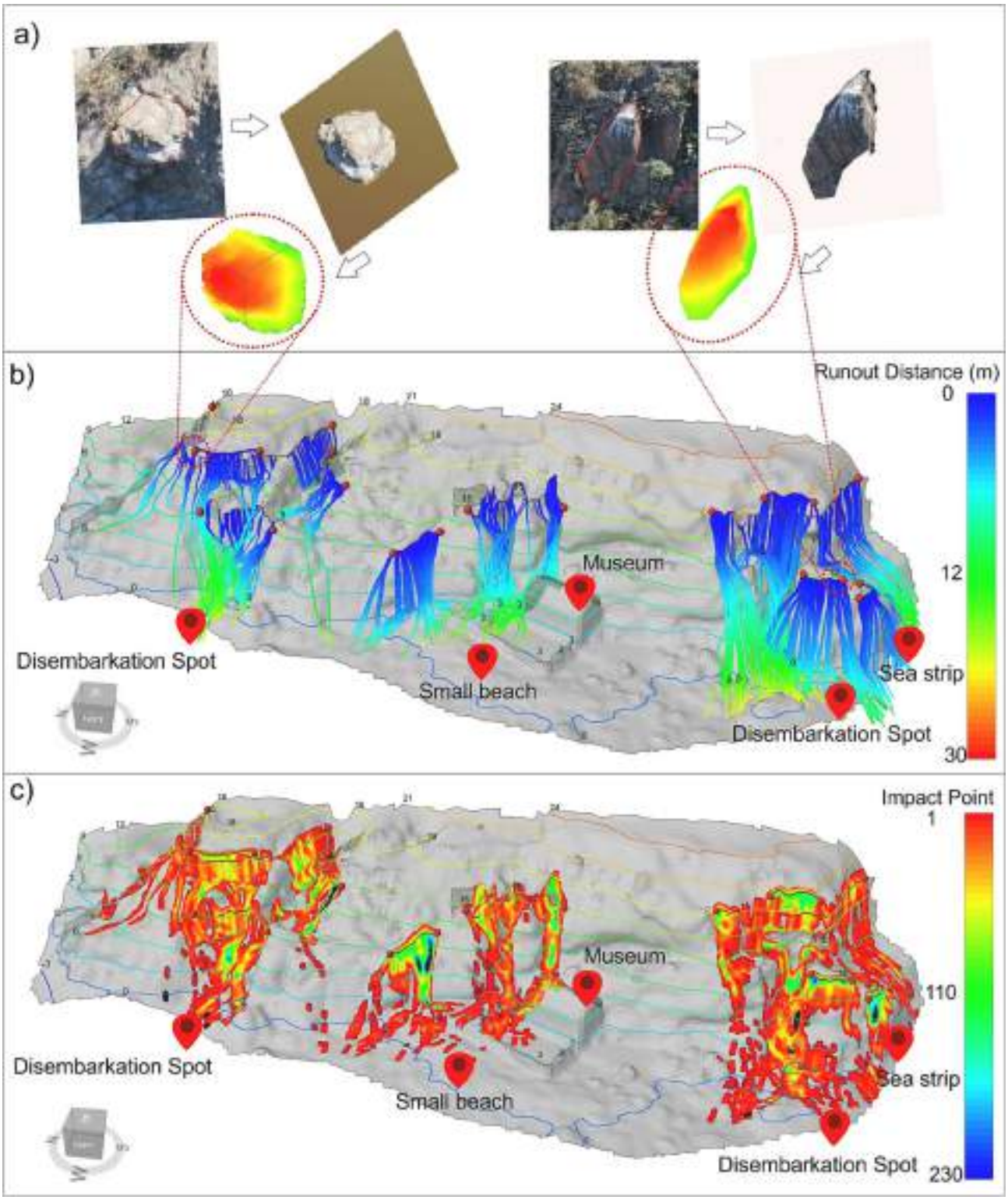

Fig. 7. a) example of boulder volume quantification on the dense point cloud; b) runout distance of simulated trajectories and main elements at risk; c) impact point of simulated trajectories and main elements at risk.

predisposing factor for rock mass failures, since it lowers the geomechanical quality through the occurrence of discontinuity sets affected by certain characteristics. One of these is the persistence, which influences the extent of pre-existing potential failure surfaces (Tuckey and Stead, 2016), thus conditioning the rock slope stability. At the studied site, the rock mass instability is driven by planar sliding, wedge sliding and toppling failure patterns. The estimated factors of safety, which were calculated by taking into account only the kinematically unstable discontinuity planes, are often lower than the limit equilibrium, with a correlated high probability of failure, thus highlighting the risk for visitors on the islet. The discontinuity shear strength parameters used herein are the most conservative, since this study is focused on the application of close-range remote sensing techniques. These, especially when applied for preliminary studies, do not allow the direct

measurement of joint field data. The numerical stability analysis results show also that the estimated factors of safety are lowered if the seismic action is considered. This proves that the rock mass stability is conditioned by the seismicity of the study area, where earthquakes can be acknowledged among the major triggering causes of landslides. Moreover, it must be underlined that the analysis carried out for this study relies also on the measurement of intact rock and discontinuity properties through laboratory tests, which allowed ascertaining the peculiarity of tested rocks. In fact, due to their geological history, lavas have a vesicular texture with voids filled by clayey material, which makes them more similar to a massive lava from the physical point of view, although being essentially a porous rock under compression. Similarly, marls have a brecciated aspect and contain numerous fragments of volcanic rocks. This aspect is relevant, because the laboratory characterization of the rock type involved in potential rockfall phenomena is often replaced using tabulated values, which in this case could have led to possible approximations in the stability model setting with specific reference to the intact rock properties. Finally, the rockfall path simulation showed that the main tourist elements on the islet have to be considered at risk, as they fall within the runout distance of simulated rockfalls (Fig. 8). These elements are the disembarkation spots, the museum and the pedestrian paths crossing the studied islet portion, along with a small beach. They represent the most likely crowded spots in case of a complete fruition of the islet, thus they have to be regarded as the main spots of concern in terms of rockfall probability of occurrence. Therefore, this study provided the knowledge of the rock mass behavior in terms of landslide threat on the islet, and the evaluation of rockfall impact on the elements at risk.

The second point of this discussion is the scientific soundness of the approach proposed herein. In fact, thanks to the technological development, the landslide survey practice increasingly relies on remote sensing technologies, even operating in close-range configuration (e.g., (Abellán et al., 2006; Caliò et al., 2023b; Gallo et al., 2021; Kong et al., 2021; Macciotta et al., 2020; Marija et al., 2022; Nikolakopoulos et al., 2022; Salvini et al., 2017; Schilirò et al., 2022; Vivaldi et al., 2023). With specific reference to this study, the use of non-contact photogrammetric surveying procedures kept proving a reliable tool when the lowest invasiveness has to be guaranteed in the survey of sub-vertical rock face, especially in protected areas. The digitally derived 3D model of the surveyed islet sector allowed analyzing in detail the unstable rock slopes, also reaching the highest sectors, where conventional surveys would have been hardly feasible. The availability of a digital rock slope model, that could be exploited also for the quantitative extraction of discontinuity orientations, was precious also to recognize the strong link between geostructural setting and tectonics at a wider scale. Moreover, the reliability of the model relies on the good georeferencing, which allowed the accurate extraction of discontinuity spatial data. However, it is always suggested to plan a field data validation campaign, to carry out comparison measurements at some spots that have already been remotely surveyed. This represents a key aspect, because the reliability of the digital model allows reducing the errors also for the quantitative estimation of rock volumes, which were estimated in the range of 0.01–1.2 m^3 at the identified source areas. Furthermore, the use of a well-sampled model for the rockfall trajectory simulation allows taking into account the morphological aspect of the threatened area, where the boulder path can suffer from abrupt variations at the expense of potential other elements at risk not previously evaluated.

The procedure that was carried out for this study can be framed also in the wide context of Nature-Based Solutions (NBS), which can be defined as adaptive measures against predicted increasing hydrometeorological hazards; these follow a holistic approach integrating both the engineering and ecosystem component in its implementation process (Kumar et al., 2020). The non-contact surveying procedures, supporting also the rock mass stability analysis, represent a reliable tool for the (1) identification of the main hazard and the (2) related impact modeling, which represent two key aspects of the NBS process.

In conclusion, the presented procedure was successful in achieving the planned goals, and its relatively easy affordability in terms of cost and management makes it repeatable in numerous other study cases worldwide.

CRediT authorship contribution statement

S. Mineo: Writing – original draft, Validation, Supervision, Project administration, Methodology, Investigation, Funding acquisition, Formal analysis, Data curation, Conceptualization. **D. Caliò:** Writing – original draft, Validation, Software, Methodology, Investigation, Formal analysis, Data curation. **G. Zocco:** Software, Investigation. **G. Pappalardo:** Writing – original draft, Validation, Supervision, Methodology, Investigation, Formal analysis, Conceptualization.

Declaration of Competing Interest

The authors declare that they have no known competing financial

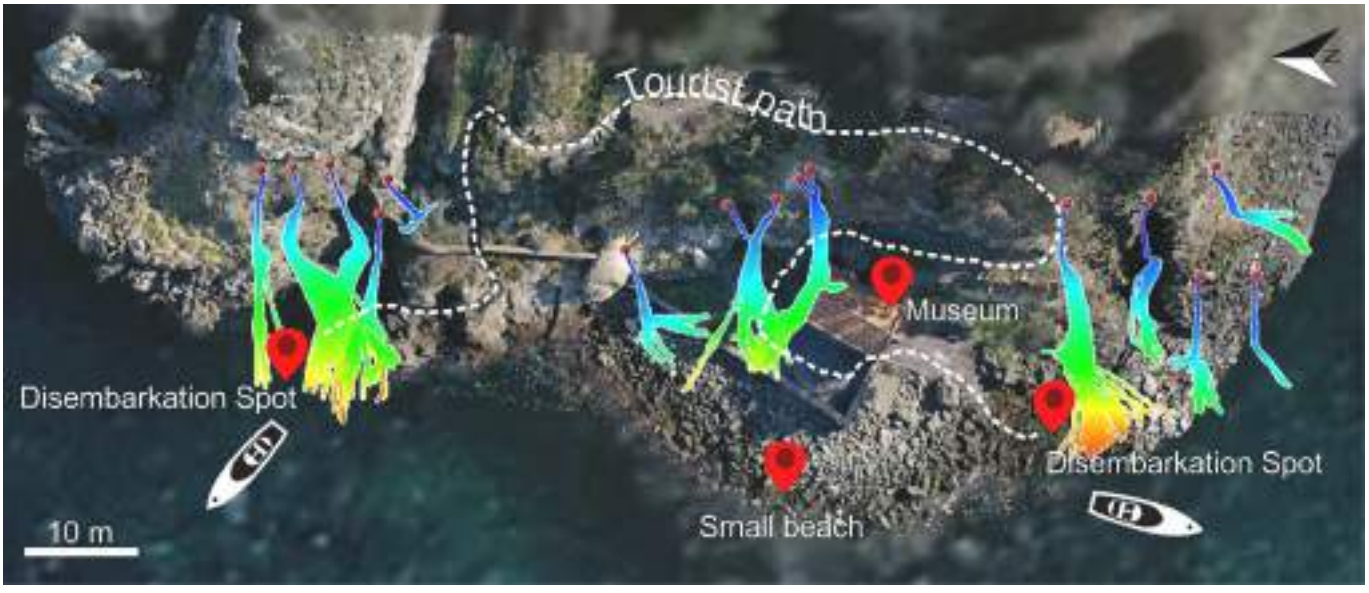

Fig. 8. Impact scenario of rockfall hazard on the main elements at risk.

interests or personal relationships that could have appeared to influence the work reported in this paper.

Data availability

The data that has been used is confidential.

Acknowledgements

This study was financially supported by University of Catania in the frame of the project: "MOdellazione Digitale di fenomeni di Instabilità di Versante attraverso procedure di telerilevamento MODIV" Piaceri linea 3 Starting Grant, Principal Investigator Simone Mineo.

Laboratory tests were carried out at the Laboratorio di Geologia Applicata of Catania University. Authors would like to thank the "Centro Universitario per la Gestione e la Tutela degli Ambienti Naturali e degli Agroecosistemi" (CUTGANA), for his support during the surveys. A particular thank is for Dr. Domenico Catalano, head of the Natural Reserve "Isola Lachea e Faraglioni dei Ciclopi", and Dr. Eng. Lucio Mannino, Director of the General Services Area of Catania University.

References

Abellán, A., Vilaplana, J.M., Martínez, J., 2006. Application of a long-range Terrestrial Laser Scanner to a detailed rockfall study at Vall de Núria (Eastern Pyrenees, Spain). Eng. Geol. 88, 136–148. https://doi.org/10.1016/j.enggeo.2006.09.012.

Agliardi, F., Crosta, G.B., 2003. High resolution three-dimensional numerical modelling of rockfalls. Int. J. Rock Mech. Min. Sci. 40, 455–471. https://doi.org/10.1016/S1365-1609(03)00021-2.

Akin, M., Dinçer, İ., Ok, A.Ö., Orhan, A., Akin, M.K., Topal, T., 2021. Assessment of the effectiveness of a rockfall ditch through 3-D probabilistic rockfall simulations and automated image processing. Eng. Geol. 283, 106001 https://doi.org/10.1016/j.enggeo.2021.106001.

Alejano, L.R., González, J., Muralha, J., 2012. Comparison of different techniques of tilt testing and basic friction angle variability assessment. Rock Mech. Rock. Eng. 45, 1023–1035. https://doi.org/10.1007/s00603-012-0265-7.

Barbano, M.S., Pappalardo, G., Pirrotta, C., Mineo, S., 2014. Landslide triggers along volcanic rock slopes in eastern Sicily (Italy). Nat. Hazards 73, 1587–1607. https://doi.org/10.1007/s11069-014-1160-1.

Barreca, G., Corradino, M., Monaco, C., Pepe, F., 2018. Active tectonics along the South East Offshore Margin of Mt. Etna: new insights from high-resolution seismic profiles. Geosciences 8, 62. https://doi.org/10.3390/geosciences8020062.

Basu, A., Mishra, D.A., Roychowdhury, K., 2013. Rock failure modes under uniaxial compression, Brazilian, and point load tests. Bull. Eng. Geol. Environ. 72, 457–475. https://doi.org/10.1007/s10064-013-0505-4.

Benjamin, J., Rosser, N.J., Brain, M.J., 2020. Emergent characteristics of rockfall inventories captured at a regional scale. Earth Surf. Process. Landf. 45, 2773–2787. https://doi.org/10.1002/esp.4929.

Bonforte, A., Guglielmino, F., Coltelli, M., Ferretti, A., Puglisi, G., 2011. Structural assessment of Mount Etna volcano from permanent scatterers analysis: structural assessment of Mount Etna. Geochem. Geophys. Geosyst. 12, n/a-n/a. https://doi.org/10.1029/2010GC003213.

Branca, S., Coltelli, M., De Beni, E., Wijbrans, J., 2008. Geological evolution of Mount Etna volcano (Italy) from earliest products until the first central volcanism (between 500 and 100 ka ago) inferred from geochronological and stratigraphic data. Int. J. Earth Sci. (Geol. Rundsch) 97, 135–152. https://doi.org/10.1007/s00531-006-0152-0.

Branca, S., De Guidi, G., Lanzafame, G., Monaco, C., 2014. Holocene vertical deformation along the coastal sector of Mt. Etna volcano (eastern Sicily, Italy): implications on the time–space constrains of the volcano lateral sliding. J. Geodyn. 82, 194–203. https://doi.org/10.1016/j.jog.2014.07.006.

Budetta, P., De Luca, C., 2015. Wedge failure hazard assessment by means of a probabilistic approach for an unstable sea-cliff. Nat. Hazards 76, 1219–1239. https://doi.org/10.1007/s11069-014-1546-0.

Caliò, D., Mineo, S., Pappalardo, G., 2023a. Digital rock mass analysis for the evaluation of rockfall magnitude at poorly accessible cliffs. Remote Sens. 15, 1515. https://doi.org/10.3390/rs15061515.

Caliò, D., Mineo, S., Pappalardo, G., 2023b. Aerial photogrammetry used as a quick procedure for rock mass stability analysis in a nature reserve. Ital. J. Eng. Geol. Environ. 1, 11. https://doi.org/10.4408/IJEGE.2023-01.S-02.

Calista, M., Mascioli, F., Menna, V., Miccadei, E., Piacentini, T., 2019. Recent geomorphological evolution and 3D numerical modelling of soft clastic rock cliffs in the Mid-Western Adriatic Sea (Abruzzo, Italy). Geosciences 9, 309. https://doi.org/10.3390/geosciences9070309.

Casagli, N., Frodella, W., Morelli, S., Tofani, V., Ciampalini, A., Intrieri, E., Raspini, F., Rossi, G., Tanteri, L., Lu, P., 2017a. Spaceborne, UAV and ground-based remote sensing techniques for landslide mapping, monitoring and early warning. Geoenviron. Disaster 4, 9. https://doi.org/10.1186/s40677-017-0073-1.

Casagli, N., Guzzetti, F., Jaboyedoff, M., Nadim, F., Petley, D., 2017b. Hydrological Risk: Landslides.

Cavallaro, D.S., 2010. Indagini Geologiche Integrate (Terra-Mare) del Bordo Orientale Emerso e Sommerso del M. Etna e Relazioni con L'evoluzione Geodinamica dell'Area. Università di Catania.

Caviezel, A., Demmel, S.E., Ringenbach, A., Bühler, Y., Lu, G., Christen, M., Dinneen, C. E., Eberhard, L.A., von Rickenbach, D., Bartelt, P., 2019. Reconstruction of four-dimensional rockfall trajectories using remote sensing and rock-based accelerometers and gyroscopes. Earth Surf. Dynam. 7, 199–210. https://doi.org/10.5194/esurf-7-199-2019.

Clemente, J.A., Spizzichino, D., Leoni, G., Marchese, A., Uriarte, J.A., Morales, T., Wilting, R., Vojinovic, Z., Faccini, F., 2023a. Rockfall susceptibility analysis through 3D simulations in marine protected areas of the Portofino coastline: case studies of San Fruttuoso and Paraggi bays. Bull. Eng. Geol. Environ. 82, 122. https://doi.org/10.1007/s10064-023-03133-3.

Clemente, J.A., Uriarte, J.A., Spizzichino, D., Faccini, F., Morales, T., 2023b. Rockfall hazard mitigation in coastal environments using dune protection: a nature-based solution case on Barinatxe beach (Basque Coast, northern Spain). Eng. Geol. 314, 107014 https://doi.org/10.1016/j.enggeo.2023.107014.

Colica, E., D'Amico, S., Iannucci, R., Martino, S., Gauci, A., Galone, L., Galea, P., Paciello, A., 2021. Using unmanned aerial vehicle photogrammetry for digital geological surveys: case study of Selmun promontory, northern of Malta. Environ. Earth Sci. 80, 551. https://doi.org/10.1007/s12665-021-09846-6.

Collins, B.D., Sitar, N., 2008. Processes of coastal bluff erosion in weakly lithified sands, Pacifica, California, USA. Geomorphology 97, 483–501. https://doi.org/10.1016/j.geomorph.2007.09.004.

Cristofolini, R., Gresta, S., Imposa, S., Menza, S., Patanè, G., 1987. An approach to problems on energy sources at Mount Etna based on seismological and volcanological data. Bull. Volcanol. 49, 729–736. https://doi.org/10.1007/BF01079824.

Daniela, R., Ermanno, M., Antonio, P., Pasquale, R., Marco, V., 2020. Assessment of Tuff Sea Cliff stability integrating geological surveys and remote sensing. Case history from Ventotene Island (Southern Italy). Remote Sens. 12, 2006. https://doi.org/10.3390/rs12122006.

Dorren, L.K.A., Berger, F., Putters, U.S., 2006. Real-size experiments and 3-D simulation of rockfall on forested and non-forested slopes. Nat. Hazards Earth Syst. Sci. 6, 145–153. https://doi.org/10.5194/nhess-6-145-2006.

Einstein, H.H., 1996. Risk and risk analysis in rock engineering. Tunn. Undergr. Space Technol. 11, 141–155. https://doi.org/10.1016/0886-7798(96)00014-4.

Fonstad, M.A., Dietrich, J.T., Courville, B.C., Jensen, J.L., Carbonneau, P.E., 2013. Topographic structure from motion: a new development in photogrammetric measurement: topographic structure from motion. Earth Surf. Process. Landf. 38, 421–430. https://doi.org/10.1002/esp.3366.

Gallo, I.G., Martínez-Corbella, M., Sarro, R., Iovine, G., López-Vinielles, J., Hérnandez, M., Robustelli, G., Mateos, R.M., García-Davalillo, J.C., 2021. An integration of UAV-based photogrammetry and 3D modelling for rockfall hazard assessment: the Cárcavos case in 2018 (Spain). Remote Sens. 13, 3450. https://doi.org/10.3390/rs13173450.

Gilham, J., Barlow, J., Moore, R., 2019. Detection and analysis of mass wasting events in chalk sea cliffs using UAV photogrammetry. Eng. Geol. 250, 101–112. https://doi.org/10.1016/j.enggeo.2019.01.013.

Goodman, R.E., Bray, J.W., 1976. Toppling of Rock Slopes. Proceedings of the Specialty Conference on Rock Engineering for Foundations and Slopes.

Hoek, E., 1973. Methods for the rapid assessment of the stability of three-dimensional rock slopes. QJEGH 6, 243–255. https://doi.org/10.1144/GSL.QJEG.1973.006.03.08.

Hoek, E., 1987. RocWall - A Program for the Analysis of Rockfalls Fiom Slopes. Department of Civil Engineering, University of Toronto, Toronto, Ontario, Canada.

Hoek, E., Bray, J.W., 1981. Rock Slope Engineering, Third Edition. ed. The Institution of Mining and Metallurgy, London.

Humphreys, J., Clark, R.W.E., 2020. A critical history of marine protected areas. In: Marine Protected Areas. Elsevier, pp. 1–12. https://doi.org/10.1016/B978-0-08-102698-4.00001-0.

James, M.R., Robson, S., 2012. Straightforward reconstruction of 3D surfaces and topography with a camera: accuracy and geoscience application: 3D surfaces and topography with a camera. J. Geophys. Res. 117, n/a–n/a. https://doi.org/10.1029/2011JF002289.

Kong, D., Saroglou, C., Wu, F., Sha, P., Li, B., 2021. Development and application of UAV-SfM photogrammetry for quantitative characterization of rock mass discontinuities. Int. J. Rock Mech. Min. Sci. 141, 104729 https://doi.org/10.1016/j.ijrmms.2021.104729.

Kriegl, M., Elías Ilosvay, X.E., von Dorrien, C., Oesterwind, D., 2021. Marine protected areas: at the crossroads of nature conservation and fisheries management. Front. Mar. Sci. 8, 676264 https://doi.org/10.3389/fmars.2021.676264.

Kumar, P., Debele, S.E., Sahani, J., Aragão, L., Barisani, F., Basu, B., Bucchignani, E., Charizopoulos, N., Di Sabatino, S., Domeneghetti, A., Edo, A.S., Finér, L., Gallotti, G., Juch, S., Leo, L.S., Loupis, M., Mickovski, S.B., Panga, D., Pavlova, I., Pilla, F., Prats, A.L., Renaud, F.G., Rutzinger, M., Basu, A.S., Shah, M.A.R., Soini, K., Stefanopoulou, M., Toth, E., Ukonmaanaho, L., Vranic, S., Zieher, T., 2020. Towards an operationalisation of nature-based solutions for natural hazards. Sci. Total Environ. 731, 138855 https://doi.org/10.1016/j.scitotenv.2020.138855.

Macciotta, R., Gräpel, C., Skirrow, R., 2020. Fragmented rockfall volume distribution from photogrammetry-based structural mapping and discrete fracture networks. Appl. Sci. 10, 6977. https://doi.org/10.3390/app10196977.

Marija, L., Martin, Z., Jordan, A., Matthew, P., 2022. Rockfall susceptibility and runout in the Valley of the Kings. Nat. Hazards 110, 451–485. https://doi.org/10.1007/s11069-021-04954-9.

Marques, F.M.S.F., 2008. Magnitude-frequency of sea cliff instabilities. Nat. Hazards Earth Syst. Sci. 8, 1161–1171. https://doi.org/10.5194/nhess-8-1161-2008.

Mineo, S., Pappalardo, G., Onorato, S., 2021. Geomechanical characterization of a rock cliff hosting a cultural heritage through ground and UAV rock mass surveys for its sustainable fruition. Sustainability 13, 924. https://doi.org/10.3390/su13020924.

Mineo, S., Caliò, D., Pappalardo, G., 2022. UAV-based photogrammetry and infrared thermography applied to rock mass survey for geomechanical purposes. Remote Sens. 14, 473. https://doi.org/10.3390/rs14030473.

Morales, T., Clemente, J.A., Damas Mollá, L., Izagirre, E., Uriarte, J.A., 2021. Analysis of instabilities in the Basque Coast Geopark coastal cliffs for its environmentally friendly management (Basque-Cantabrian basin, northern Spain). Eng. Geol. 283, 106023 https://doi.org/10.1016/j.enggeo.2021.106023.

Nikolakopoulos, K.G., Kyriou, A., Koukouvelas, I.K., 2022. Developing a guideline of unmanned aerial vehicle's acquisition geometry for landslide mapping and monitoring. Appl. Sci. 12, 4598. https://doi.org/10.3390/app12094598.

Noël, F., Jaboyedoff, M., Caviezel, A., Hibert, C., Bourrier, F., Malet, J.-P., 2022. Rockfall trajectory reconstruction: a flexible method utilizing video footage and high-resolution terrain models. Earth Surf. Dynam. 10, 1141–1164. https://doi.org/10.5194/esurf-10-1141-2022.

Pappalardo, G., Mineo, S., 2017. Investigation on the mechanical attitude of basaltic rocks from Mount Etna through InfraRed Thermography and laboratory tests. Constr. Build. Mater. 134, 228–235. https://doi.org/10.1016/j.conbuildmat.2016.12.146.

Pappalardo, G., Mineo, S., Monaco, C., 2016. Geotechnical characterization of limestones employed for the reconstruction of a UNESCO world heritage Baroque monument in southeastern Sicily (Italy). Eng. Geol. 212, 86–97. https://doi.org/10.1016/j.enggeo.2016.08.004.

Pappalardo, G., Punturo, R., Mineo, S., Contrafatto, L., 2017. The role of porosity on the engineering geological properties of 1669 lavas from Mount Etna. Eng. Geol. 221, 16–28. https://doi.org/10.1016/j.enggeo.2017.02.020.

Pappalardo, G., Mineo, S., Carbone, S., Monaco, C., Catalano, D., Signorello, G., 2021. Preliminary recognition of geohazards at the natural reserve "Lachea Islet and Cyclop Rocks" (Southern Italy). Sustainability 13, 1082. https://doi.org/10.3390/su13031082.

Park, H.-J., West, T.R., Woo, I., 2005. Probabilistic analysis of rock slope stability and random properties of discontinuity parameters, Interstate Highway 40, Western North Carolina, USA. Eng. Geol. 79, 230–250. https://doi.org/10.1016/j.enggeo.2005.02.001.

Pfeiffer, T.J., Bowen, T.D., 1989. Computer simulation of rockfalls. Environ. Eng. Geosci. xxvi, 135–146. https://doi.org/10.2113/gseegeosci.xxvi.1.135.

Pfeiffer, T.J., Higgins, J.D., 1990. Rockfall hazard analysis using the colorado rock£all simulation program. Transp. Res. Rec. 117–126.

Porter, N.J., Trenhaile, A.S., 2007. Short-term rock surface expansion and contraction in the intertidal zone. Earth Surf. Process. Landf. 32, 1379–1397. https://doi.org/10.1002/esp.1479.

Quevauviller, P., Gemmer, M., 2015. EU and international policies for hydrometeorological risks: operational aspects and link to climate action. Adv. Clim. Chang. Res. 6, 74–79. https://doi.org/10.1016/j.accre.2015.09.002.

Radhi, M.S.M., Pauzi, N.I.M., Omar, H., 2008. Probabilistic approach of rock slope stability analysis using Monte Carlo simulation. ICCBT 37, 449–468.

Rosser, N.J., Brain, M.J., Petley, D.N., Lim, M., Norman, E.C., 2013. Coastline retreat via progressive failure of rocky coastal cliffs. Geology 41, 939–942. https://doi.org/10.1130/G34371.1.

Salvini, R., Mastrorocco, G., Seddaiu, M., Rossi, D., Vanneschi, C., 2017. The use of an unmanned aerial vehicle for fracture mapping within a marble quarry (Carrara, Italy): photogrammetry and discrete fracture network modelling. Geomat. Nat. Haz. Risk 8, 34–52. https://doi.org/10.1080/19475705.2016.1199053.

Schilirò, L., Robiati, C., Smeraglia, L., Vinci, F., Iannace, A., Parente, M., Tavani, S., 2022. An integrated approach for the reconstruction of rockfall scenarios from UAV and satellite-based data in the Sorrento Peninsula (southern Italy). Eng. Geol. 308, 106795 https://doi.org/10.1016/j.enggeo.2022.106795.

Stimpson, B., 1981. A suggested technique for determining the basic friction angle of rock surfaces using core. Int. J. Rock Mech. Min. Sci. Geomech. Abstr. 18, 63–65. https://doi.org/10.1016/0148-9062(81)90266-7.

Sturzenegger, M., Stead, D., 2009. Close-range terrestrial digital photogrammetry and terrestrial laser scanning for discontinuity characterization on rock cuts. Eng. Geol. 106, 163–182. https://doi.org/10.1016/j.enggeo.2009.03.004.

Tanguy, J.-C., Condomines, M., Kieffer, G., 1997. Evolution of the Mount Etna magma: constraints on the present feeding system and eruptive mechanism. J. Volcanol. Geotherm. Res. 75, 221–250. https://doi.org/10.1016/S0377-0273(96)00065-0.

Tokiwa, T., Tsusaka, K., Ishii, E., Sanada, H., Tominaga, E., Hatsuyama, Y., Funaki, H., 2011. Influence of a fault system on rock mass response to shaft excavation in soft sedimentary rock, Horonobe area, northern Japan. Int. J. Rock Mech. Min. Sci. 48, 773–781. https://doi.org/10.1016/j.ijrmms.2011.04.007.

Tonkin, T., Midgley, N., 2016. Ground-control networks for image based surface reconstruction: an investigation of optimum survey designs using UAV derived imagery and structure-from-motion photogrammetry. Remote Sens. 8, 786. https://doi.org/10.3390/rs8090786.

Tu, Y.-H., Johansen, K., Aragon, B., Stutsel, B.M., Angel, Y., Camargo, O.A.L., Al-Mashharawi, S.K.M., Jiang, J., Ziliani, M.G., McCabe, M.F., 2021. Combining Nadir, Oblique, and Façade imagery enhances reconstruction of rock formations using unmanned aerial vehicles. IEEE Trans. Geosci. Remote Sens. 59, 9987–9999. https://doi.org/10.1109/TGRS.2020.3047435.

Tuckey, Z., Stead, D., 2016. Improvements to field and remote sensing methods for mapping discontinuity persistence and intact rock bridges in rock slopes. Eng. Geol. 208, 136–153. https://doi.org/10.1016/j.enggeo.2016.05.001.

Vivaldi, V., Bordoni, M., Mineo, S., Crozi, M., Pappalardo, G., Meisina, C., 2023. Airborne combined photogrammetry—infrared thermography applied to landslide remote monitoring. Landslides 20, 297–313. https://doi.org/10.1007/s10346-022-01970-z.

Wang, C.-H., Fang, L., Chang, D.T.-T., Huang, F.-C., 2023. Back-analysis of a rainfall-induced landslide case history using deterministic and random limit equilibrium methods. Eng. Geol. 317, 107055 https://doi.org/10.1016/j.enggeo.2023.107055.

Westoby, M.J., Brasington, J., Glasser, N.F., Hambrey, M.J., Reynolds, J.M., 2012. 'Structure-from-Motion' photogrammetry: a low-cost, effective tool for geoscience applications. Geomorphology 179, 300–314. https://doi.org/10.1016/j.geomorph.2012.08.021.

Wheaton, J.M., Brasington, J., Darby, S.E., Sear, D.A., 2009. Accounting for uncertainty in DEMs from repeat topographic surveys: improved sediment budgets. Earth Surf. Process. Landf. https://doi.org/10.1002/esp.1886 n/a-n/a.

Willenberg, H., Loew, S., Eberhardt, E., Evans, K.F., Spillmann, T., Heincke, B., Maurer, H., Green, A.G., 2008. Internal structure and deformation of an unstable crystalline rock mass above Randa (Switzerland): part I — Internal structure from integrated geological and geophysical investigations. Eng. Geol. 101, 1–14. https://doi.org/10.1016/j.enggeo.2008.01.015.

Wyllie, D.C., Mah, C., 2014. Rock Slope Engineering: Fourth Edition, 4th ed. CRC Press, London.

Yan, J., Chen, J., Tan, C., Zhang, Y., Liu, Y., Zhao, X., Wang, Q., 2023. Rockfall source areas identification at local scale by integrating discontinuity-based threshold slope angle and rockfall trajectory analyses. Eng. Geol. 313, 106993 https://doi.org/10.1016/j.enggeo.2023.106993.

Young, A.P., 2018. Decadal-scale coastal cliff retreat in southern and Central California. Geomorphology 300, 164–175. https://doi.org/10.1016/j.geomorph.2017.10.010.

Zhang, N., Li, C.C., Lu, A., Chen, X., Liu, D., Zhu, E., 2019. Experimental studies on the basic friction angle of planar rock surfaces by tilt test. J. Test. Eval. 47, 20170308. https://doi.org/10.1520/JTE20170308.

Zhang, W., Zhao, X., Pan, X., Wei, M., Yan, J., Chen, J., 2022. Characterization of high and steep slopes and 3D rockfall statistical kinematic analysis for Kangyuqu area, China. Eng. Geol. 308, 106807 https://doi.org/10.1016/j.enggeo.2022.106807.